APS physics

CHORUS

This is the accepted manuscript made available via CHORUS. The article has been published as:

Ionization in collisions between metastable hydrogen atoms

Alex Bohr, Andrew Blickle, Stephen Paolini, Luke Ohlinger, and Robert C. Forrey

Phys. Rev. A **85**, 042710 — Published 11 April 2012

DOI: 10.1103/PhysRevA.85.042710

Ionization in collision between metastable hydrogen atoms

Alex Bohr, Andrew Blickle, Stephen Paolini, Luke Ohlinger, and Robert C. Forrey*

Penn State University, Berks Campus, Reading, PA 19610-6009

(Received:)

Abstract

Associative and Penning ionization cross sections are calculated for collisions between metastable hydrogen 2s atoms at thermal energies. Cross sections for deuterium 2s collisions are also reported. The associative ionization cross sections behave as E^{-1} for collision energy E, in agreement with an existing experiment. The Penning ionization cross sections dominate for all energies and are found to follow the $E^{-2/3}$ behavior that was predicted in previous work for the total ionization cross section. The magnitudes of our theoretical associative ionization cross sections for H(2s)+H(2s) collisions are between two and four times larger than the experimental data.

*Corresponding author: rcf6@psu.edu

I. INTRODUCTION

Associative ionization is the most elementary bond-forming process that can occur during a collision of two atoms. The translational energy of the colliding atoms is transferred into kinetic energy of the ejected electron leaving the positively charged molecular ion in its ground or excited rovibrational state. This process has been studied for metastable hydrogen atom collisions with various targets [1–7] including ground state hydrogen atoms where it provides a mechanism which is believed to contribute to the formation of H_2^+ in astrophysical environments that are not in local thermodynamic equilibrium. These include protostellar outflows [8], envelopes of supernovae [9], and stellar atmospheres [10–12]. The inverse process of dissociative recombination of H_2^+ is also known to be important in many astrophysical environments and due to its technological importance has been the subject of extensive theoretical [13–22] and experimental [23–34] investigations. Associative ionization between two metastable hydrogen atoms is less likely to occur naturally due to competition with other reactions. Nevertheless, the process is of fundamental interest and has been studied experimentally [6]. To our knowledge, there have been no theoretical studies reported for associative ionization between two metastable hydrogen atoms. Theoretical results have been reported [35] for associative ionization due to colliding pairs of excited helium atoms. This system is similar to the case of metastable hydrogen but considerably more complex. The theoretical simplicity of hydrogen makes it ideal for studying fundamental physics and offers an opportunity to gain better insights into the collisional dynamics.

Production of cold metastable hydrogen atoms [36–40] also opens the door to a variety of possible applications including the development of a Lyman-α laser [38,40], the use of H(2s) atoms as a diagnostic in Bose-Einstein condensation [41–43], and improved accuracy in the determination of fundamental constants [44]. An important prerequisite for achieving the goal of high-resolution spectroscopy of metastable hydrogen is a detailed understanding of the atomic collisions. The mutual destruction of 2s atoms in collisions limits the density of metastable atoms that can be achieved. This limit has implications for schemes that use slow beams of D(2s) atoms in a deuterium atomic parity violation experiment [45]. The process

may also be important in the interpretation of precision measurements of the two-photon transition frequency [46]. Collisional production of fast metastable hydrogen atoms from cold H_2 has recently been demonstrated [47] and may also lead to important applications.

Once formed, collisional quenching of pairs of H(2s) atoms may occur through either of the associative and Penning ionization reactions:

$$\mathrm{H}(2s) + \mathrm{H}(2s) \rightarrow \mathrm{H}_2^+ + e^- \tag{1}$$

$$\mathrm{H}(2s) + \mathrm{H}(2s) \rightarrow \mathrm{H}(1s) + \mathrm{H}^+ + e^- \tag{2}$$

or via the single and double excitation transfer reactions:

$$\mathrm{H}(2s) + \mathrm{H}(2s) \rightarrow \mathrm{H}(2s) + \mathrm{H}(2p) \tag{3}$$

$$\mathrm{H}(2s) + \mathrm{H}(2s) \rightarrow \mathrm{H}(2p) + \mathrm{H}(2p) \tag{4}$$

and likewise for D(2s) reactions. The competitive balance between the collisional quenching processes (1)–(4) should be understood at the highest possible level of detail. A series of calculations [48–52] have addressed this issue and provided theoretical benchmarks for this fundamental system. However, the calculated trap loss rate coefficients are about 4 times larger than the experimental values and show little temperature variation in the 100-200 μK region where the experiment suggests there may be a significant decrease [39]. At such low collision energies, there are many considerations that complicate the calculations including spin-orbit, hyperfine, and non-adiabatic radial and angular couplings. At thermal energies, these couplings become negligible, and it should be easier to gain insight into the ionization part of the collisional quenching process. Additionally, there is experimental data [6] for the associative ionization contribution that may be directly compared against.

The associative ionization process (1) competes with the Penning ionization process (2). Both reactions are highly exothermic with ΔE ranging from 6.8 eV for Penning ionization to 9.45 eV for associative ionization into the ground rovibrational state. The large number of open final states effectively forms a complete set which justifies the use of a local potential formulation. At the energies considered in the present work, the energy splitting between the 2s and 2p states may be neglected which allows the dynamics of the ionization to be

studied using only a single complex potential energy curve. The bound and continuum rovibrational wave functions are computed using a square integrable Sturmian basis set. The positive energy pseudostates provide a discretized representation of the H_2^+ continuum. Transitions to bound states are summed over to obtain the associative ionization cross section. Likewise, transitions to the positive energy pseudostates are summed over to obtain the Penning cross section. The completeness of the rovibrational basis set is measured by adding the associative and Penning ionization cross sections together and comparing with the cross section obtained by using the unitarity property of the S-matrix. The sum rule is found to be well-satisfied for metastable hydrogen and deuterium systems. Numerical results for $^1\Sigma_g^+$ and $^3\Sigma_u^+$ symmetries are reported for H(2s)+H(2s), D(2s)+D(2s), and H(2s)+D(2s) collisions, and comparisons are made with a Langevin model and an experiment [6] over a wide range of energies.

II. THEORY

A pair of 2s hydrogen atoms may approach in either a $^1\Sigma_g^+$ or a $^3\Sigma_u^+$ molecular state. Since the 2s and 2p states are nearly degenerate, the molecular interaction strongly couples the atomic product state $\phi_{2s}\phi_{2s}$ with $\phi_{2s}\phi_{2p}$ and $\phi_{2p}\phi_{2p}$ states of the same molecular symmetry. States with different molecular symmetry are also coupled due to the spin-orbit interaction. The full set of doubly excited molecular states converging to the H(n=2)+H(n'=2) limit, the so-called Q(2) states, has been calculated over the entire range of internuclear distance R, and the associated energies and autoionization widths have been used to construct complex potential curves [49,51]. Multichannel scattering formulations have been used to calculate the collision cross sections at low translational energies [48,50]. At thermal energies, the tiny energy splitting between the 2s and 2p states may be ignored, and the contribution from the Coriolis force is also expected to be weak. Therefore, it is possible to simplify the analysis by considering only single channel scattering on the complex potentials $V_\pm(R)$ which have the asymptotic behavior [48]

$$V_\pm(R) \sim \pm\frac{C_3}{R^3} + O(R^{-5}) \tag{5}$$

where $C_3 = 9\sqrt{6}$ and the energy is in atomic units. In this formulation, the wave function describing the approach of one 2s atom on nuclei a with another 2s atom on nuclei b will contain the incident plane wave

$$\phi_{2s}(a)\phi_{2s}(b)\, e^{i\vec{k}\cdot\vec{R}} = \frac{1}{\sqrt{2}}\left(\xi^+ + \xi^-\right)\, e^{i\vec{k}\cdot\vec{R}} \tag{6}$$

where k is the translational wave number, and $\xi^{\pm}$ are molecular eigenfunctions associated with the $V_{\pm}(R)$ potentials. The molecular eigenfunctions tend to linear combinations of atomic $\phi_{2s}\phi_{2s}$ and $\phi_{2p}\phi_{2p}$ product states as $R \to \infty$, and the incident wave function (6) evolves into

$$\Psi(\vec{R}) \sim \frac{1}{\sqrt{2}}\left(\xi^+ + \xi^-\right)\, e^{i\vec{k}\cdot\vec{R}} + \frac{1}{\sqrt{2}}\left[\xi^+ f^{(+)}(\theta,\phi) + \xi^- f^{(-)}(\theta,\phi)\right]\, \frac{e^{ikR}}{R} \tag{7}$$

where

$$f^{(\pm)}(\theta) = \frac{1}{2ik}\sum_{l=0}^{\infty}(2l+1)(e^{2i\delta_l^{(\pm)}} - 1)P_l(\cos\theta) \tag{8}$$

is the amplitude for scattering through an angle θ by the complex interaction potential $V_{\pm}$. The complex phase shift $\delta_l^{(\pm)}$ contains information about the ionization. The differential cross sections for elastic scattering may be obtained from the coefficient of the spherical wave part of the wave function (7) by expressing the molecular eigenfunctions in terms of their asymptotic atomic states. The result is [48]

$$\frac{d\sigma_{2s2s\to 2s2s}}{d\Omega} = \frac{1}{4}\left|f^{(+)}(\theta,\phi) + f^{(-)}(\theta,\phi)\right|^2 \tag{9}$$

$$\frac{d\sigma_{2s2s\to 2p2p}}{d\Omega} = \frac{1}{4}\left|f^{(+)}(\theta,\phi) - f^{(-)}(\theta,\phi)\right|^2 \tag{10}$$

It is assumed in this analysis that coupling to the single excitation transfer channel $\phi_{2s}\phi_{2p}$, which vanishes at leading order in an expansion in inverse powers of R, may be neglected. Recent investigations [51] have shown that significant nonadiabatic coupling to $\phi_{2s}\phi_{2p}$ may occur at higher order due to the dipole-quadrupole interaction, and that this coupling can have a significant effect on the cross sections at very low energies [52]. In the present work, however, we consider sufficiently high energies where the contribution from $\phi_{2s}\phi_{2p}$ coupling

is expected to be small. We tested this assumption for the lowest energies considered in this work and found no significant change in the total ionization cross section when the $\phi_{2s}\phi_{2p}$ coupling is neglected. At this level of approximation, the total ionization cross section may be obtained from equations (9) and (10) to be

$$\sigma_{ion} = \frac{\pi}{k^2}\sum_{l=0}^{\infty}(2l+1)\left[1 - A_l^2\right] \tag{11}$$

$$A_l^2 = \sum_f |S_{if}^{(l)}|^2 = \tfrac{1}{2}\left(|A_l^+|^2 + |A_l^-|^2\right) \tag{12}$$

where $S_{if}^{(l)}$ is the scattering matrix connecting initial and final channels for partial wave l. The absorption factors $A_l^{\pm}$ are determined by the imaginary components of the complex phase shifts $\delta_l^{(\pm)}$ and may be obtained by solving the Schrödinger equation for the two potentials $V_{\pm}(R)$.

A "Langevin" model based only on the long-range part of the potentials $V_{\pm}(R)$ is useful to gain insight into the dynamics of the reaction. Ionization generally occurs when the translational energy is greater than the potential energy barrier. The long-range part of $V_+(R)$ repels the atoms so that $A_l^+ = 1$ for all l. This immediately reduces the opacity by a factor of two as may be readily seen from equations (11) and (12). The contribution from $V_-(R)$ may be estimated by considering the effective potential

$$V_{\text{eff}}(R) = \frac{l(l+1)}{2\mu R^2} - \frac{C_3}{R^3} \tag{13}$$

where μ is the reduced mass of the system. Differentiating V_{eff} with respect to R and setting it to zero yields the location R_0 and energy $E = V_{\text{eff}}(R_0)$ of the barrier in terms of the angular momentum. The opacity is expected to drop sharply at this value of angular momentum which allows a convenient truncation of the sum in equation (11). Assuming a unit step function opacity and dividing by two to account for the long-range repulsive potential contribution yields the total ionization cross section

$$\sigma_{ion} = \frac{3\pi}{2}\left(\frac{C_3}{2E}\right)^{2/3} \sim 23\,E^{-2/3} \quad \text{a.u.} \tag{14}$$

Previous calculations [48,50] have shown that the total ionization cross sections for the $^1\Sigma_g^+$ and $^3\Sigma_u^+$ states are $23E^{-2/3}$ and $15E^{-2/3}$, respectively.

The above discussion may be modified to account for identical nuclei by allowing the translational part of the incident wave function to be $\frac{1}{\sqrt{2}}[\exp(i\vec{k}\cdot\vec{R}) \pm \exp(-i\vec{k}\cdot\vec{R})]$ which introduces a factor of $\frac{1}{\sqrt{2}}[1 \pm (-1)^l]$ to the partial wave scattering amplitude due to the rotational parity of the Legendre polynomial $P_l[\cos(\pi-\theta)] = (-1)^l P_l(\cos\theta)$ in equation (8). The total ionization cross section (11) is then modified to

$$\sigma_{ion} = \frac{\pi}{2k^2} \sum_{l=0}^{\infty} w_l \, (2l+1) \left[1 \pm (-1)^l\right]^2 \left[1 - A_l^2\right] \tag{15}$$

where w_l accounts for the nuclear spin statistics and the $\pm$ signs are determined by the requirement that the total wave function be antisymmetric under interchange of the nuclei. Note that this $\pm$ is not related to the notation that was used above to specify the $V_\pm$ potentials. In order to avoid confusion, we remove the $\frac{1}{2}[1 \pm (-1)^l]^2$ factor in equation (15) and write the cross section as twice the sum over even or odd l. The choice of even/odd and the statistical weights are determined by the molecular symmetry of the potential used to compute the opacity. For example, hydrogen atoms in a spin-polarized gas would interact only through states of ${}^3\Sigma_u^+$ symmetry and have $w_l = 1$ for even l and $w_l = 0$ for odd l. For a hydrogen gas with a statistical mixture of nuclear spins, the cross sections are

$$\sigma_{ion}^S = \frac{\pi}{k^2} \left(\tfrac{1}{4} \sum_{l=even} + \tfrac{3}{4} \sum_{l=odd} \right) (2l+1) \left(1 - |A_l^-(S)|^2\right) \tag{16}$$

$$\sigma_{ion}^T = \frac{\pi}{k^2} \left(\tfrac{3}{4} \sum_{l=even} + \tfrac{1}{4} \sum_{l=odd} \right) (2l+1) \left(1 - |A_l^-(T)|^2\right) \tag{17}$$

where the opacities are calculated using the complex $V_-(R)$ potential with the appropriate ${}^1\Sigma_g^+$ or ${}^3\Sigma_u^+$ symmetry. The electron spins introduce additional statistical weights so that the total ionization cross section is given by

$$\sigma_{ion} = \tfrac{1}{4}\sigma_{ion}^S + \tfrac{3}{4}\sigma_{ion}^T \ . \tag{18}$$

The total ionization cross section computed from the direct solution of the Schrödinger equation together with the unitarity properties of the S-matrix must be equal to the sum of the individual final state contributions. In the present work, the individual contributions

coming from associative and Penning ionization are calculated from the solution to the inhomogeneous differential equation

$$\left[-\frac{1}{2\mu}\frac{d^2}{dR^2}+\frac{l(l+1)}{2\mu R^2}+V_-(R)-E\right]\psi_l(R)=\chi_{vj}(R)\left[\frac{\Gamma(R)}{2\pi}\right]^{1/2} \tag{19}$$

where $\chi_{vj}(R)$ is the ro-vibrational wave function of the discrete state (or pseudostate) of the H_2^+ molecule, and $\Gamma(R)$ is the autoionization width which is equal to twice the negative of the imaginary part of $V_-(R)$. Energy conservation yields $E=\frac{k_e^2}{2}+\epsilon_{vj}-6.8$ eV where k_e is the electron momentum and ϵ_{vj} is the ro-vibrational energy. The wave function is energy-normalized according to the asymptotic form

$$\psi_l(R)\sim\sqrt{\tfrac{2\mu}{\pi k}}\,e^{i\delta_l}\sin(kr-\tfrac{l\pi}{2}+\delta_l)\ . \tag{20}$$

If the 2s hydrogen atoms approach in the $^1\Sigma_g^+$ molecular state, then the emitted electron must have even angular momentum, and the transition will obey the selection rule $j=l$. If the atoms approach in the $^3\Sigma_u^+$ state, then the emitted electron must have odd angular momentum, and the transition will obey the selection rule $j=l\pm1$ in order to preserve the overall ungerade symmetry. Therefore, the cross sections are given by

$$\sigma_{vj}^S=\frac{2\pi^2}{k^2}\,w_j\,(2j+1)\,\left|\langle\psi_j|\Gamma^{1/2}|\chi_{vj}\rangle\right|^2 \tag{21}$$

$$\sigma_{vj}^T=\frac{2\pi^2}{k^2}\,w_j\,\left[(j+1)\,\left|\langle\psi_{j+1}|\Gamma^{1/2}|\chi_{vj}\rangle\right|^2+j\,\left|\langle\psi_{j-1}|\Gamma^{1/2}|\chi_{vj}\rangle\right|^2\right] \tag{22}$$

where w_j equals $\frac{1}{4}$ for even j and $\frac{3}{4}$ for odd j. We note that the equation (22) is the same as that used by Bieniek and Dalgarno [53] for the analogous problem of associative detachment in collisions of H and H^-. For a statistical mixture of singlet and triplet molecular states, the associative and Penning ionization cross sections are given by

$$\sigma_A=\sum_{j=0}^{j_{max}}\sum_{v=0}^{n_j}\left(\tfrac{1}{4}\sigma_{vj}^S+\tfrac{3}{4}\sigma_{vj}^T\right) \tag{23}$$

$$\sigma_P=\sum_{j=0}^{j_{max}}\sum_{v=n_j+1}^{v_{max}}\left(\tfrac{1}{4}\sigma_{vj}^S+\tfrac{3}{4}\sigma_{vj}^T\right) \tag{24}$$

where n_j is the index of the last bound vibrational level for the rotational level j. The dissociative continuum is described by pseudostates with $v > n_j$. The bound ro-vibrational wave functions and the continuum pseudostates are obtained by diagonalization of the H_2^+ Hamiltonian in the orthonormal Laguerre polynomial basis set

$$\phi_{l,n}(R) = \sqrt{\frac{an!}{(n+2l+2)!}}\,(aR)^{l+1}\exp(-aR/2)L_n^{(2l+2)}(aR) \tag{25}$$

The inhomogeneous differential equation (19) is solved using the renormalized Numerov method [54]. The sum of σ_A and σ_P computed using equations (23) and (24) is compared with the total cross section computed using equation (18).

III. RESULTS

The calculations were performed using the potential curves shown in Figure 1. The H(2s)+H(2s) curves were taken from previous work [49,51] and the H_2^+ curve was obtained from the code of Aubert-Frecon et al. [55]. The repulsive wall for the $^3\Sigma_u^+$ state occurs at a larger separation than that of the $^1\Sigma_g^+$ state. Therefore, we would expect more efficient ionization to occur for 2s atoms that approach on the $^1\Sigma_g^+$ state. This expectation was observed in our calculations and will be discussed in detail below.

Convergence tests were performed with respect to v_{max}, j_{max}, and the Laguerre scale parameter a for both singlet and triplet symmetries. Not surprisingly, the sensitivity to the scale parameter a is much greater for Penning ionization than for associative ionization. Figure 2 shows the scale dependence for $^1\Sigma_g^+$ calculations for three collision energies. The Penning ionization cross sections are stationary for $a = 14 - 16$, so we chose $a = 15$ for the full calculations. Figure 3 shows the convergence pattern of the j-th partial cross section as a function of j for the $^1\Sigma_g^+$ state at a collision energy of 0.001 a.u. The inhomogeneous curve was computed by solving the inhomogeneous Schrödinger equation (19) followed by a summation over both associative and Penning ionization contributions for $v \leq 50$. Also shown is the homogeneous solution to the Schrödinger equation which automatically includes both ionization contributions. The plot shows that the two methods of solution are in

excellent agreement for large-j. To bring the small-j results into the same level of agreement requires an increase in v_{max}. We have found that $v_{max} = j_{max} = 100$ produces converged results for the inhomogeneous problem (as measured by the very good agreement of the summed cross section compared with the homogeneous solution) for all of the collision energies considered in this work.

The sharp drop in the partial cross section seen in Figure 3 is a general feature of ionization in collisions between metastable hydrogen atoms. It occurs when the centrifugal barrier is large enough to prevent the atoms from a close approach where ionization can take place. The angular momentum where the sharp decrease in the partial cross section occurs may be estimated using the formula

$$j = (54\mu^3 C_3^2 E)^{1/6} \tag{26}$$

which is obtained from the Langevin model. This equation predicts that the sharp decrease will occur at $j = 52$ for $E = 0.001$ a.u. which is in good agreement with the location seen in Figure 3. The oscillatory behavior in the figure is due to the nuclear spin statistical factor w_j which depends on whether j is even or odd. This factor also depends on the isotopic partner assumed in the collision. In this work, we considered metastable hydrogen and deuterium collisions. The results are summarized below.

A. H(2s)+H(2s)

Figure 4 shows the associative and Penning ionization cross sections for hydrogen atoms approaching on the $^1\Sigma_g^+$ molecular state over a broad range of energies. Also shown in the figure are energy-dependent fits to the theoretical data which are seen to be in good agreement. The E^{-1} dependence of the associative ionization cross section follows directly from the prefactor of equation (21). The $E^{-2/3}$ dependence of the Penning cross section shows that the exact numerical solution to equation (19) agrees very well with the Langevin model (14) and confirms that all atoms that cross the centrifugal barrier will react.

The reaction probability is not unity when the centrifugal barrier is surmounted for hydrogen atoms approaching on a $^3\Sigma_u^+$ molecular state. In this case, there are two separate

terms that contribute to equation (22), and in both cases, the probability for ionization is reduced due to the location of the inner repulsive wall (see Figure 1). The energy dependence, however, continues to follow E^{-1} and $E^{-2/3}$ behavior for a wide range of energies as shown in Figure 5. Although the Penning cross section is reduced for the $^3\Sigma_u^+$ case, both of the associative ionization contributions to equation (22) are approximately equal, and their sum is approximately the same as the cross section for the $^1\Sigma_g^+$ case.

For an unpolarized gas, a statistical mixture of singlet and triplet molecular states is assumed which yield the cross sections given in equations (23) and (24). The results are shown in Figure 6 along with the experimental data of Urbain et al. [6] for associative ionization. The comparison shows that our theoretical calculations are within a factor of two with experiment at high energies and within a factor of four at the lower energies considered. It is interesting that the discrepancy between the present theory and experiment is approximately the same as the one seen previously for the same system at much lower energies [52].

B. D(2s)+D(2s)

For deuterium atoms, the nuclear spin statistical factor w_j equals $\frac{2}{3}$ for even j and $\frac{1}{3}$ for odd j. At thermal energies, this difference in spin statistics compared to hydrogen atoms does not have a significant effect. Figure 7 shows the associative and Penning ionization cross sections for a pair of D(2s) atoms. The Penning ionization cross section for D(2s) atoms approaching on the $^1\Sigma_g^+$ state is identical to the result for H(2s). These collisions are governed by the same conditions that led to equation (14) where there is no reduced mass dependence. The Penning ionization for the $^3\Sigma_u^+$ state is larger than the value for hydrogen but still less than the Langevin limit with unit reaction probability. Unlike hydrogen, the associative ionization cross section for the $^3\Sigma_u^+$ state of deuterium is approximately two times larger than that of the $^1\Sigma_g^+$ state, and both cross sections are smaller than their corresponding values for hydrogen. The energy-dependent fitting functions are included in the figure for each state.

C. H(2s)+D(2s)

Figure 8 shows the ionization cross sections for H(2s)+D(2s) and again confirms that there is no reduced mass dependence in the Penning ionization cross section for the $^1\Sigma_g^+$ state. For the $^3\Sigma_u^+$ state, the Penning cross section lies in between that of H(2s)+H(2s) and D(2s)+D(2s) and the reduced mass scaling was found to follow the approximate formula

$$\sigma_P(\mu) = \sigma_P(H_2) \left[\frac{\mu}{\mu_{H_2}}\right]^{1/4} \tag{27}$$

for $0.5 \leq \mu \leq 1.5$. The associative ionization cross sections for the $^3\Sigma_u^+$ and $^1\Sigma_g^+$ states are nearly the same for H(2s)+D(2s), similar to what was found for H(2s)+H(2s). The magnitude of the associative cross sections lie in between that of H(2s)+H(2s) and D(2s)+D(2s), but unlike the Penning cross section, they tend to decrease with increasing reduced mass. The ratio

$$R(\mu) = \frac{\sigma_A(\mu)}{\sigma_A(H_2)} \left[\frac{\mu}{\mu_{H_2}}\right]^{3/2} \tag{28}$$

was used to scale the associative ionization cross sections to that of hydrogen. Figure 9 shows that the scaling ratio is a good approximation to unity for the $^1\Sigma_g^+$ state but not for the $^3\Sigma_u^+$ state. This observation shows that it is not possible to find a reduced mass scaling formula for the associative cross section when the opacity deviates from a unit step function.

IV. SUMMARY

Associative and Penning ionization cross sections have been calculated for H(2s)+H(2s), D(2s)+D(2s), and H(2s)+D(2s) collisions at thermal energies. Excellent agreement is found between the summed state-to-state cross sections and the total cross section obtained from direct solution of the Schrödinger equation. This agreement confirms the validity of the closure approximation and justifies the use of the local complex potential formulation for these collision partners. The E^{-1} energy dependence of the associative ionization cross section agrees with an existing experiment [6]. However, the magnitude of our theoretical cross sections are found to be about 2-4 times larger than the experimental data over a

wide range of energies. This discrepancy is consistent with one seen previously at ultracold energies and suggests that there may be a systematic oversight in the theoretical formulation.

In an effort to uncover possible oversights in the theory, we have reviewed in detail the coupled states scattering formulation that was used in our calculations. We have also tested the assumption that the ionization is insensitive to non-adiabatic radial coupling by expanding the basis set to include the $\phi_{2s}\phi_{2p}$ state. Consistent with previous calculations at ultracold energies [52] we find some changes in the relative contributions from the single and double excitation transfer reactions (3) and (4) but no change in the total ionization cross section. Inclusion of the fine structure and Lamb shift energy defects also produced no significant changes at high energies. Another possible source of the discrepancy is the neglect in our calculations of the Coriolis interaction when solving the Schrödinger equation in the body-fixed frame. Previous calculations [52] attempted to deal with this issue by transforming from molecular gauge to atomic gauge where the uncalculated non-adiabatic angular terms have the proper long-range fall-off. This procedure uncovered some sensitivity to short-range radial couplings that are negligible within the coupled states approximation. Our expectation, however, is that Coriolis coupling to the $\phi_{2s}\phi_{2s}$ state should be weak and become even less important with increasing energy. Figure 6 appears to support the second part of our expectation as the discrepancy changes from a factor of 4 at low energy to a factor of 2 at the higher energies. This issue requires further investigation.

As a concluding remark, we note that our calculations provide detailed cross sections for the formation of $H_2^+(v, j)$ for all vibrational and rotational levels. If the theoretical formulation is indeed responsible for the discrepancy discussed above, it is possible that the relative state selected cross sections may still be reliable. If the ejected electron energy spectra could be measured as in the case of metastable helium atom collisions [35], then the theory given here could be further constrained.

Acknowledgments

This work was supported by National Science Foundation Grant No. PHY-0854838.

REFERENCES

[1] V. Dose, W. Hett, R. E. Olson, P. Pradel, F. Roussel, A. S. Schlachter, and G. Spiess, Phys. Rev. A 12, 1261 (1975).

[2] V. Dose and A. Richard, J. Phys. B 14, 63 (1981).

[3] D. Fussen, W. Claeys, A. Cornet, J. Jureta and P. Defrance, J. Phys. B 15, L715 (1982).

[4] W. Claeys, A. Cornet, V. Lorent, J. Jureta, and D. Fussen, J. Phys. B 19, 2955 (1986)

[5] X. Urbain, A. Cornet, F. Brouillard, and A. Giusti-Suzor, PRL 66, 1685 (1991) .

[6] X. Urbain, A. Cornet, and J. Jureta, J. Phys. B **25**, L189 (1992).

[7] B. G. Brunetti, S. Falcinelli, E. Giaquinto, A. Sassara, M. Prieto-Manzanares, and F. Vecchiocattivi, Phys. Rev. A 52, 855 (1995).

[8] J. M. Rawlings, J. E. Drew, and M. J. Barlow, MNRAS 265, 968 (1993).

[9] S. Miller, J. Tennyson, S. Lepp, and A. Dalgarno, Nature 355, 420 (2002).

[10] A. A. Mihajlov, D. Jevremovic, P. Hauschildt, M. S. Dimitrijevic, L. M. Ignjatovi, and F. Alard, A&A 403, 787 (2003).

[11] A. A. Mihajlov, D. Jevremovic, P. Hauschildt, M. S. Dimitrijevic, L. M. Ignjatovi, and F. Alard, A&A 471, 671 (2007).

[12] A. A. Mihajlov, L. M. Ignjatovi, V. A. Srekovi, and . S. Dimitrijevi, ApJS 193, 2 (2011).

[13] A. Giusti-Suzor, J. N. Bardsley, and C. Derkits, Phys. Rev. A 28 682 (1983).

[14] K. Nakashima, H. Takagi, and H. Nakamura, J. Chem. Phys. 86 726 (1987).

[15] A. P. Hickman, J. Phys. B 20 2091 (1987).

[16] I. F. Schneider, O. Dulieu, and A. Giusti-Suzor, J. Phys. B 24 L289 (1991).

[17] H. Takagi, J. Phys. B 26 4815 (1993).

[18] M. G. Golubcov, G. V. Golubcov, and G. K. Ivanov, J. Phys. B 30, 5511 (1997).

[19] V. Ngassam, O. Motapon, A. Florescu, L. Pichl, I. F. Schneider, and A. Suzor-Weiner, Phys. Rev A 68 032704 (2003).

[20] O. Motapon, F. O. Waffeu-Tamo, X. Urbain, and I. F. Schneider, Phys. Rev. A 77 052711 (2008).

[21] H. Takagi, S. Hara, and H. Sato, J. Phys.: Conf. Ser. 192 012003 (2009).

[22] M Fifirig and M Stroe, J. Phys. B 44 085202 (2011).

[23] G. H. Dunn and B. Van Zyl, Phys. Rev. 154 40 (1967).

[24] B. Peart and K. T. Dolder, J. Phys. B 7 236 (1974).

[25] J. Wm. McGowan, R. Caudano, and J. Keyser, Phys. Rev. Lett. 36 1447 (1976).

[26] A. Sen, J. Wm. McGowan, and J. B. A. Mitchell, J. Phys. B 20 1509 (1987).

[27] H. Hus, F. Yousif, C. Noren, A. Sen, and J. B. A. Mitchell, PRL 60 1006 (1988).

[28] H. T. Schmidt, L. Vejby-Christensen, H. B. Pedersen, D. Kella, N. Bjerre, and L. H. Andersen, J. Phys. B 29 2485 (1996).

[29] W. J. van der Zande, J. Semaniak, V. Zengin, G. Sundstrom, S. Rosen, C. Stromholm, S. Datz, H. Danared, and M. Larsson, Phys. Rev. A 54 5010 (1996).

[30] L. H. Andersen, P. J. Johnson, D. Kella, H. B. Pedersen, and L. Vejby-Christensen, Phys. Rev. A 55 2799 (1997).

[31] T. Tanabe, H. Takagi, I. Katayama, K. Chida, T. Watanabe, Y. Arakaki, Y. Haruyama, M. Saito, I. Nomura, T. Honma, K. Noda, and K. Hosono, PRL 83 2163 (1999).

[32] M. Saito, Y. Haruyama, T. Tanabe, I. Katayama, K. Chida, T. Watanabe, Y. Arakaki, I. Nomura, T. Honma, K. Noda, and K. Hosono, Phys. Rev. A 61 062707 (2000).

[33] S. Krohn, Z. Amitay, A. Baer, D. Zajfman, M. Lange, L. Knoll, J. Levin, D. Schwalm, R. Wester, and A. Wolf A, Phys. Rev. A 62 032713 (2000).

[34] M. O. Abdellahi El Ghazaly, J. Jureta, X. Urbain, and P. Defrance, JPB 37 2467 (2004).

[35] M. W. Muller, A. Merz, M.-W. Ruf, H. Hotop, W. Meyer, and M. Movre, Z. Phys. D 21, 89 (1991).

[36] K. Harvey, J. Appl. Phys. **53**, 3383 (1982).

[37] N. E. Rothery and E. A. Hessels, Phys. Rev. A **61**, 044501 (2000).

[38] L. P. Yatsenko, B. W. Shore, T. Halfmann, K. Bergmann, and A. Vardi, Phys. Rev. A **60**, R4237 (1999).

[39] D. Landhuis, L. Matos, S. C. Moss, J. K. Steinberger, K. Vant, L. Willmann, T. J. Greytak, and D. Kleppner, Phys. Rev. A **67**, 022718 (2003).

[40] L. P. Yatsenko, V. I. Romanenko, B. W. Shore, T. Halfmann, and K. Bergmann, Phys. Rev. A **71**, 033418 (2005).

[41] D. G. Fried, T. C. Killian, L. Willmann, D. Landhuis, S. C. Moss, D. Kleppner, and T. J. Greytak, Phys. Rev. Lett. **81**, 3811 (1998).

[42] C. L. Cesar, D. G. fried, T. C. Killian, A. D. Polcyn, J. C. Sandberg, I. A. Yu, T. J. Greytak, D. Kleppner, and J. M. Doyle, Phys. Rev. Lett. **77**, 255 (1996).

[43] T. C. Killian, D. G. Fried, L. Willmann, D. Landhuis, S. C. Moss, T. J. Greytak, and D. Kleppner, Phys. Rev. Lett. **81**, 3807 (1998).

[44] L. Willmann and D. Kleppner, *The hydrogen atom: precision physics of simple atomic systems*, edited by S. G. Karshenboim et al. (Springer-Verlag, Berlin, 2001), p. 42.

[45] R. W. Dunford and R. J. Holt, J. Phys. G: Nucl. Part. Phys. **34**, 2099 (2007).

[46] N. Kolachevsky, M. Fisher, S. G. Karshenboim, and T. W. Hänsch, Phys. Rev. Lett. **92**, 033003 (2004).

[47] A. Medina, G. Rahmat, C. R. deCarvalho, G. Jalbert, F. Zappa, R. F. Nascimento, R. Cireasa, N. Vanhaecke, I. F. Schneider, N. V. de Castro Faria, and J. Robert, J. Phys.

B **44**, 215203 (2011).

[48] R. C. Forrey, R. Cote, A. Dalgarno, S. Jonsell, A. Saenz, and P. Froelich, Phys. Rev. Lett. **85**, 4245 (2000).

[49] S. Jonsell, A. Saenz, P. Froelich, R. C. Forrey, R. Cote, and A. Dalgarno, Phys. Rev. A **65**, 042501 (2002).

[50] R. C. Forrey, S. Jonsell, A. Saenz, P. Froelich, and A. Dalgarno, Phys. Rev. A **67**, 040701R (2003).

[51] Y. V. Vanne, A. Saenz, A. Dalgarno, R. C. Forrey, P. Froelich, and S. Jonsell, Phys. Rev. A **73**, 062706 (2006).

[52] R. C. Forrey, A. Dalgarno, Y. V. Vanne, A. Saenz, and P. Froelich, Phys. Rev. A **76**, 052709 (2007).

[53] R. J. Bieniek and A. Dalgarno, ApJ **228**, 635 (1979).

[54] J. P. Leroy and R. Wallace, J. Phys. Chem. **89**, 1928 (1985).

[55] M. Aubert-Frecon, G. Hadinger, and A. Yanacopoulo, J. Phys. B **22**, 2427 (1989).

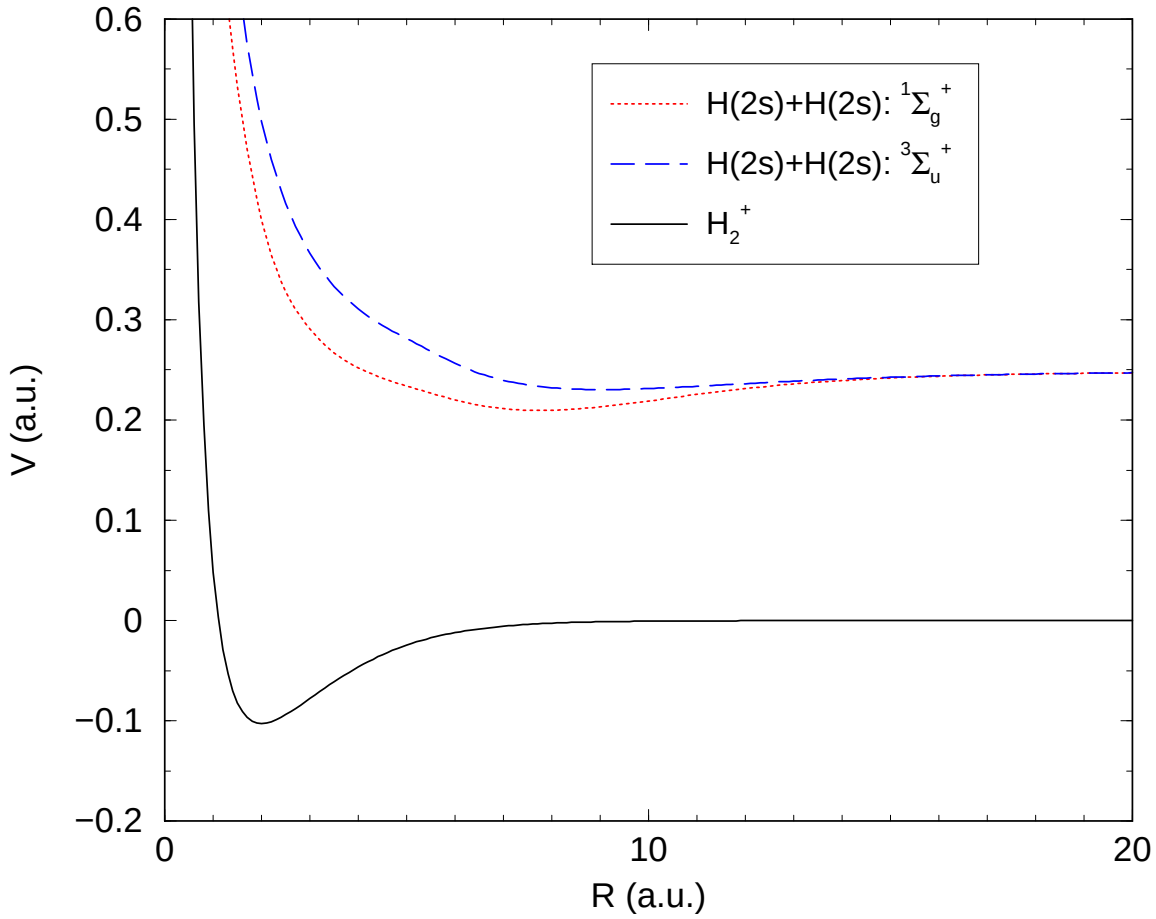

Figure 1: (Color online) Potential curves used to compute the ionization cross sections. The H(2s)+H(2s) potentials also have imaginary components which were reported in [49].

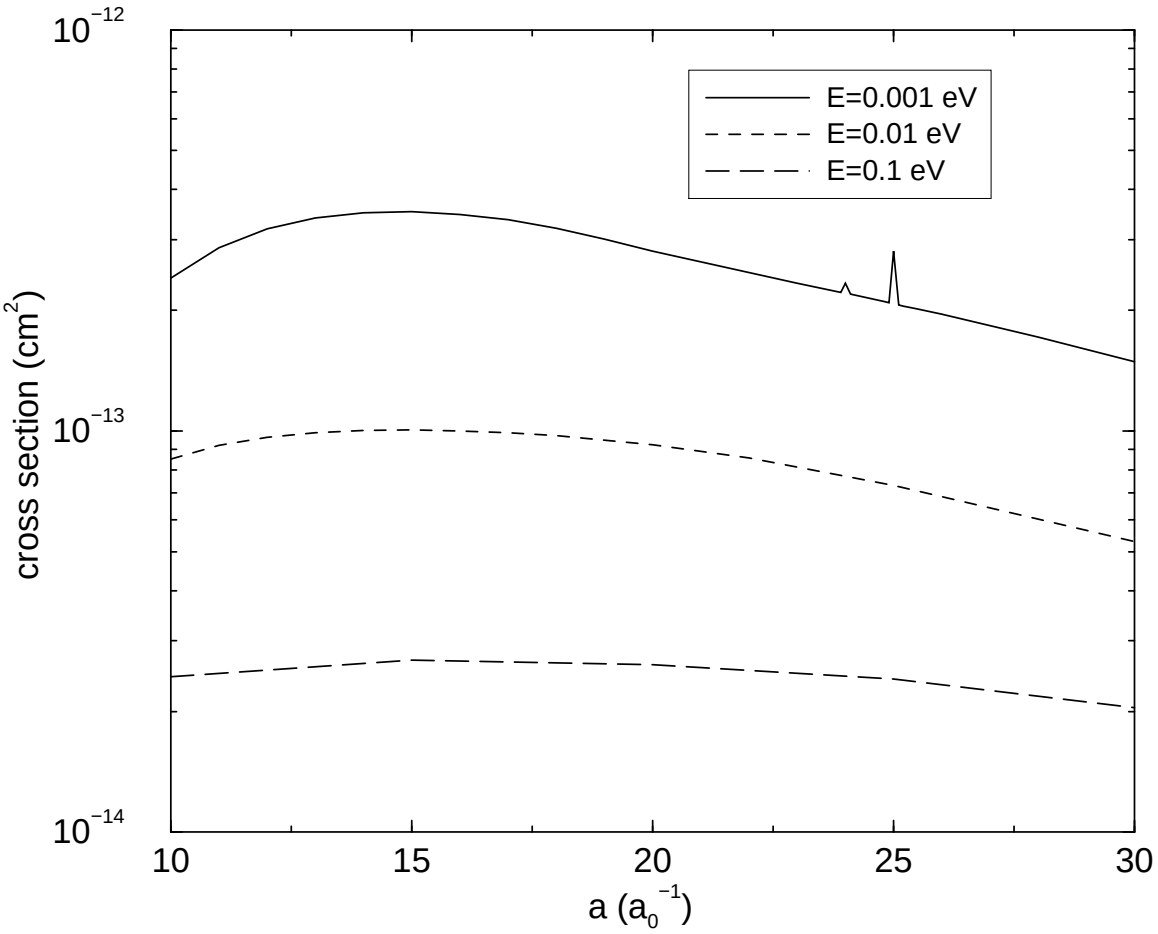

Figure 2: Penning ionization cross sections as a function of Laguerre polynomial length scale a. The associative ionization cross sections are numerically well-converged for the range $10 < a < 30$ and are not shown. The Penning cross section is stationary with $a = 15$ for all energies considered in this work.

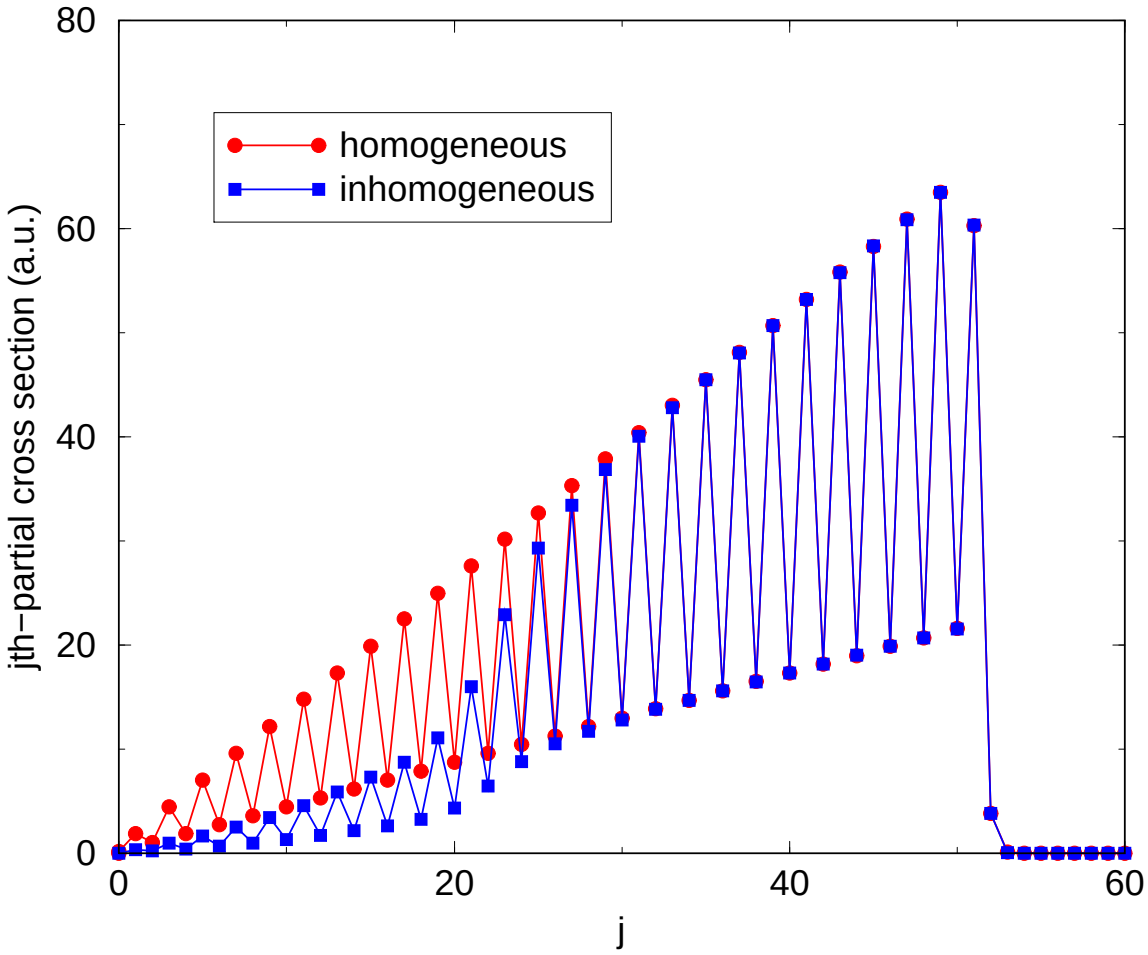

Figure 3: (Color online) Total ionization cross section at $E = 0.001$ a.u. The inhomogeneous curve was computed by solving equation (19) and adding the associative and Penning contributions for $v \leq 50$. The homogeneous curve was computed by direct solution of the Schrödinger equation. The convergence with v is generally slower for small-j. Increasing the upper limit to $v_{max} = 100$ brings the two curves into excellent agreement for all j.

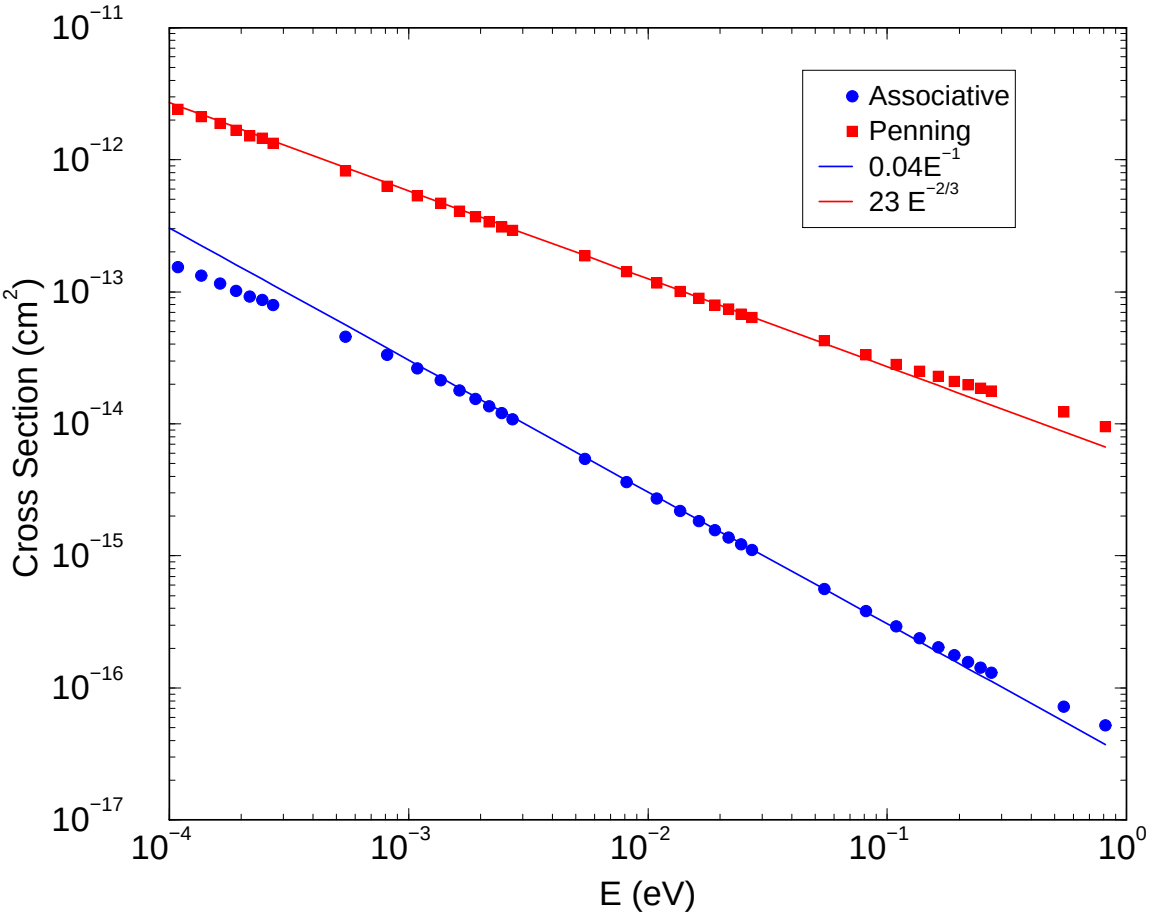

Figure 4: (Color online) Associative and Penning ionization cross sections for H(2s)+H(2s) approaching on the $^1\Sigma_g^+$ state. Also included is a curve fit ($0.04E^{-1}$) to the associative ionization cross section and a curve fit ($23E^{-2/3}$) to the Penning ionization cross section. These calculations include all contributions for $v_{max} = 100$ and $j_{max} = 100$.

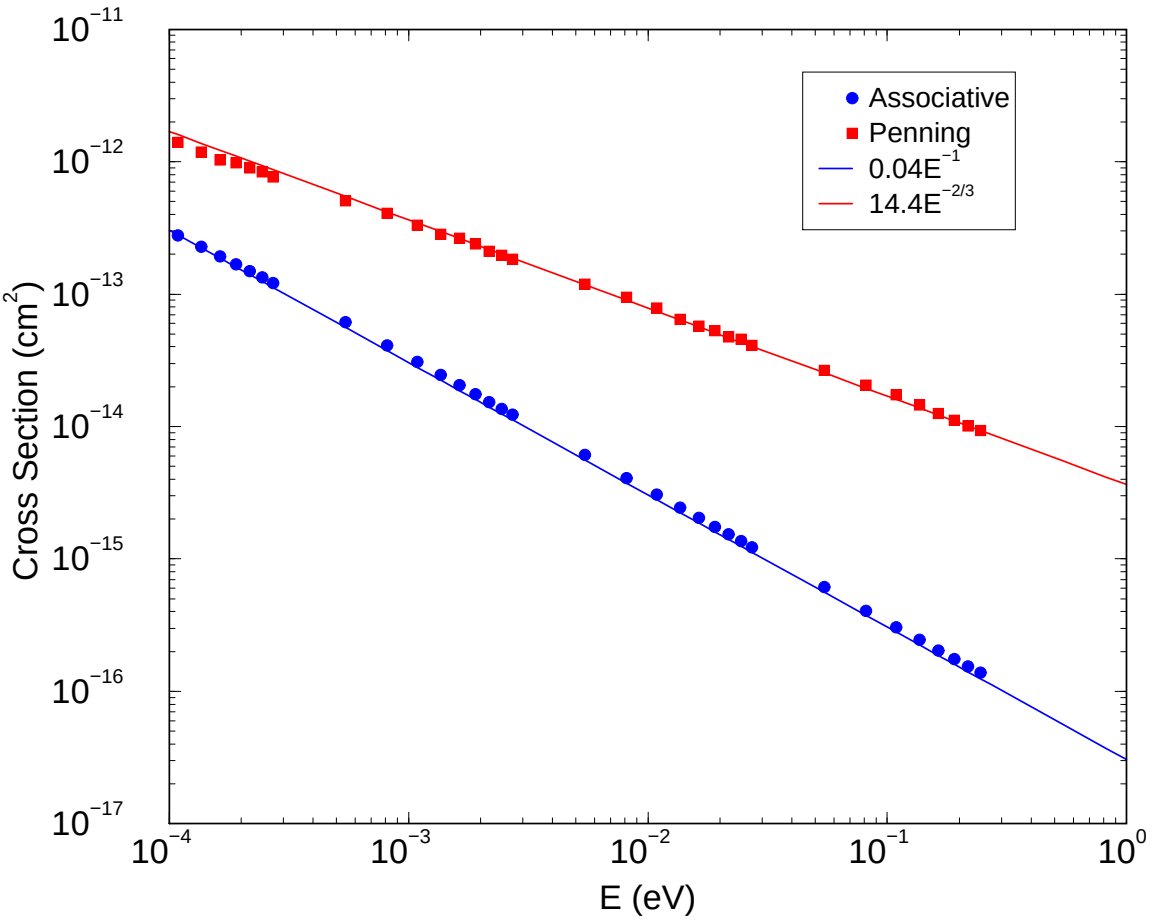

Figure 5: (Color online) Associative and Penning ionization cross sections for H(2s)+H(2s) approaching on the $^3\Sigma_u^+$ state. Also included is a curve fit ($0.04E^{-1}$) to the associative ionization cross section and a curve fit ($14.4E^{-2/3}$) to the Penning ionization cross section. These calculations include all contributions for $v_{max} = 100$ and $j_{max} = 100$.

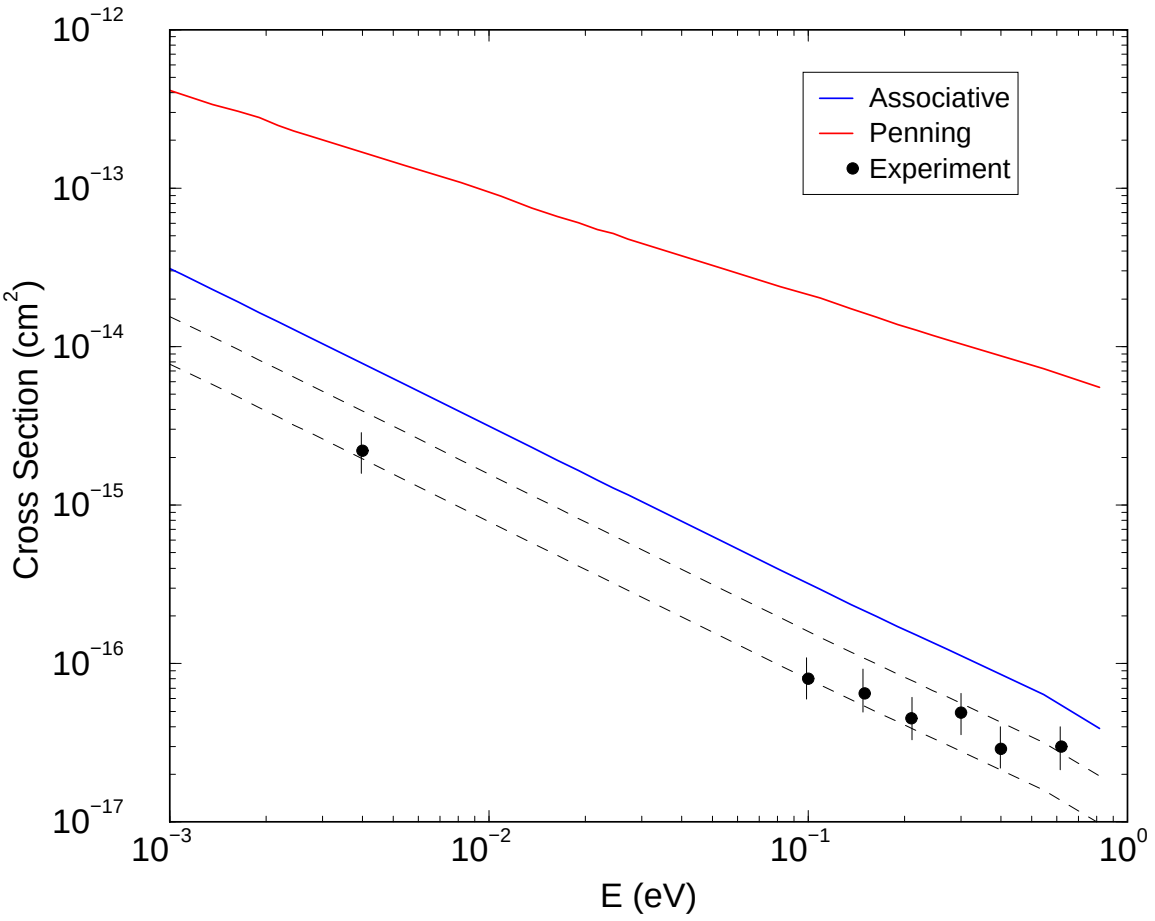

Figure 6: (Color online) Associative and Penning ionization cross sections for unpolarized H(2s)+H(2s) collisions. The experimental data is taken from Urbain et al. [6] for associative ionization. All of the experimental data lies within the dashed curves, which were obtained by dividing our theoretical associative ionization cross sections by 2 and 4.

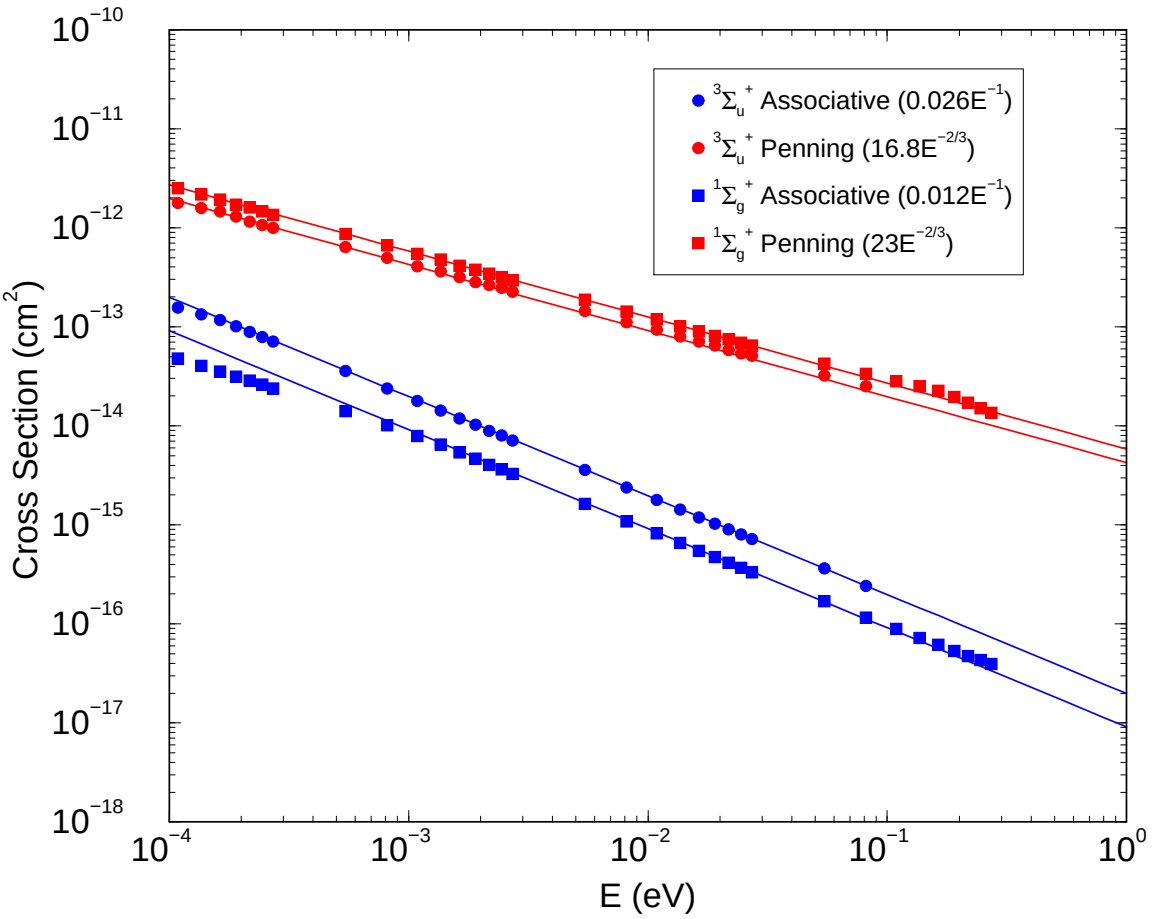

Figure 7: (Color online) Associative and Penning ionization cross sections for D(2s)+D(2s) collisions. Energy-dependent fits to the data are given in the legend and plotted as solid lines on the graph.

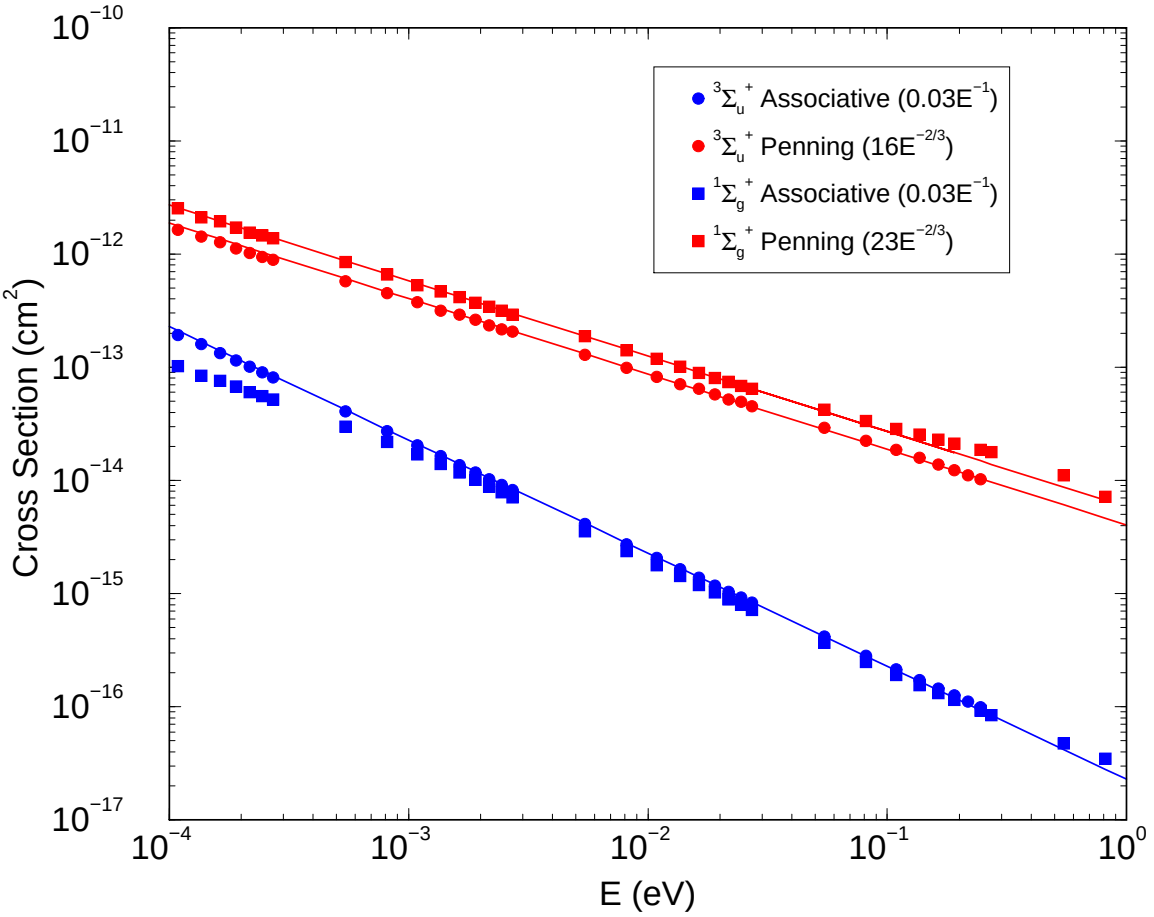

Figure 8: (Color online) Associative and Penning ionization cross sections for H(2s)+D(2s) collisions. Energy-dependent fits to the data are given in the legend and plotted as solid lines on the graph.

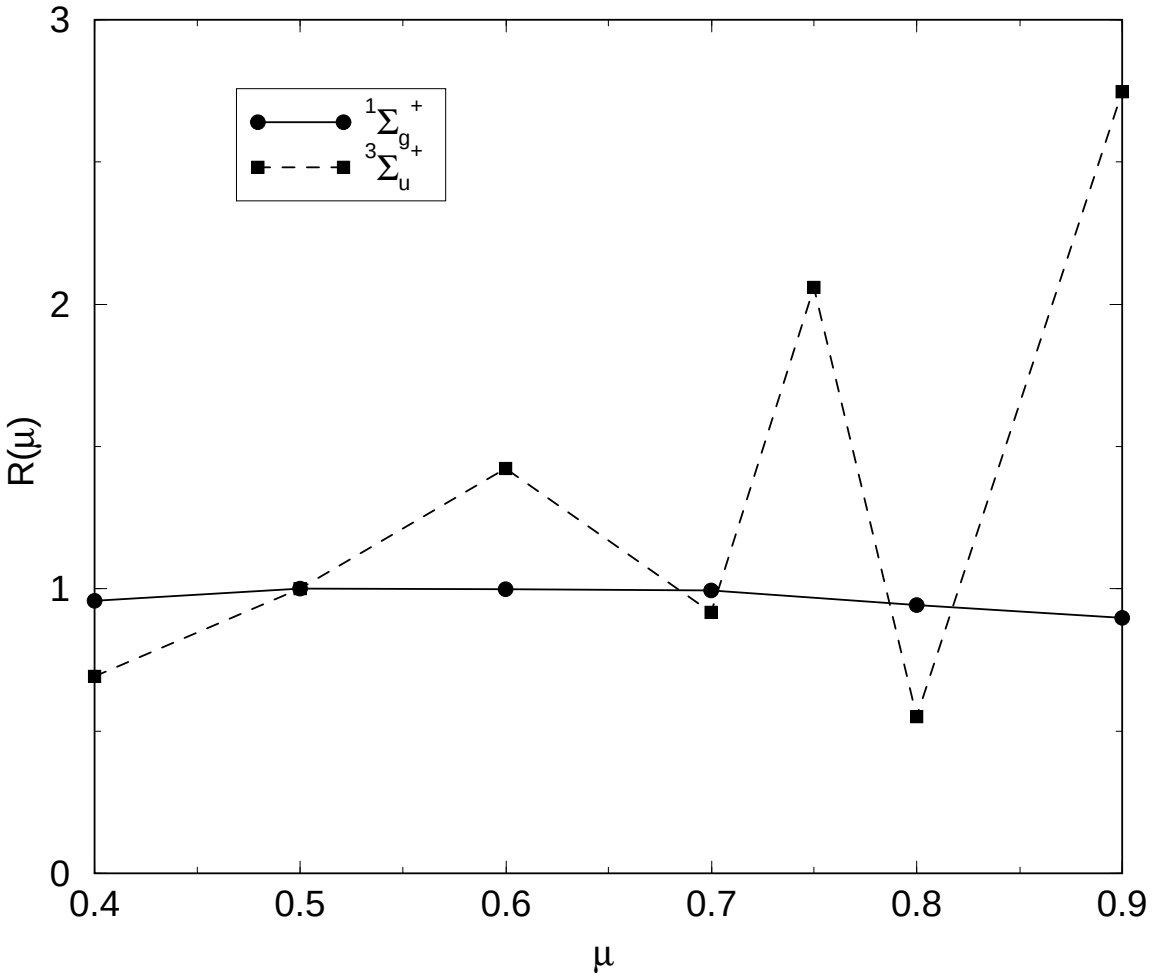

Figure 9: $R(\mu)$ versus μ for $^1\Sigma_g^+$ and $^3\Sigma_u^+$ states. These results show that a reduce mass scaling formula may be obtained for $^1\Sigma_g^+$ but not for $^3\Sigma_u^+$ states.